

# Many Body Density of States of a system of non interacting fermions

Rémi Lefèvre, Krissia Zawadzki, and Grégoire Ithier  
*Department of Physics, Royal Holloway University of London\**

The description of out-of-equilibrium many-body systems requires to go beyond the low-energy physics and local densities of states. Many-body localization, presence or lack of thermalization and quantum chaos are examples of phenomena in which states at different energy scales, including the highly excited ones, contribute to the dynamics and therefore affect the system's properties. Quantifying these contributions requires the many-body density of states (MBDoS), a function whose calculation becomes challenging even for non-interacting identical quantum particles due to the difficulty in enumerating states while enforcing the exchange symmetry. In the present work, we introduce a new approach to evaluate the MBDoS in the case of systems that can be mapped into free fermions. The starting point of our method is the principal component analysis of the filling matrix  $F$  describing how  $N$  fermions can be configured into  $L$  single-particle energy levels. We show that the many body spectrum can be expanded as a weighted sum of universal spectra given by the principal components of the filling matrix. The weighting coefficients only involve renormalized energies obtained from the single body spectrum. We illustrate our method in two classes of problems that are mapped into spinless fermions: (i) non-interacting electrons in a homogeneous tight-binding model in 1D and 2D, and (ii) interacting spins in a chain under a transverse field.

## I. INTRODUCTION

The concept of Density of States (DoS) is at the heart of statistical physics where it defines partition function and temperature. In nuclear physics, quantifying the level density is necessary to describe nuclear reactions involving excited states [1]. No less importantly, it is one of the most appealing quantity in condensed matter physics, where one is interested in investigating how electrons and holes populate energy bands to give rise to material's properties [2]. In all these fields, the density of states is crucial to characterize a multi-particle system and determine which states are accessible at energy scales of interest.

For a long time, the success of mean field theories and the quasi-particle picture to describe a highly degenerate Fermi liquid has promoted the Single-Body Local Density of States (SBLDoS) to the focus of investigations of electronic systems. In the presence of interactions, efforts have been concentrated in the physics at low temperatures, so that the LDoS around the Fermi level suffices to obtain most of their properties. Nonetheless, the quest of calculating a *Many-Body* Density of States (MBDoS) has become arguably necessary in the context of isolated quantum systems undergoing an out-of-equilibrium dynamics [3]. There, contributions from different parts of the spectrum prevents one from relying on a description based solely on the low-lying states and on the SBLDoS. Quantifying these contributions is crucial to shed light on phenomena such as quantum chaos [4], thermalization and its lack [5–7], many-body localization [8] and more generally unconventional stationary states [9, 10].

In this respect, a MBDoS provides useful information, as it allows for quantifying how interactions between indi-

vidual constituents lead to a complex many-body dynamics, with coexisting single-particle and collective effects. Even non-interacting systems pose a challenge due to the combinatorial nature of the problem of how single-body levels can be populated to define a distribution of many-body energy levels. For both non-interacting and interacting systems, it is possible to retrieve the full spectrum of energies and eigenstates only for system sizes that do not exceed a dozen of particles. Symmetries can aid this calculation by allowing one to split the total Hilbert space in blocks, associated with the projection of the Hamiltonian into states with conserved quantum numbers. This idea has served as the basis of exact diagonalization [11], and it is also implemented in well established numerical methods, as for instance the Kernel Polynomial Method (KPM) [12]. In the context of nuclear physics, methods to calculate the MBDoS started with Bethe [13] with a Fermi gas approximation, and inspired approaches such as the constant temperature [1] or the continuum shell model [14]. More involved methods using exact combinatorial counting [15, 16], recursive relations [17], or saddle approximations [18] provided some approximate results.

The calculation of the MBDoS is the problem at the focus of the present paper. We propose a new approach to calculate the exact MBDoS based on the symmetries of a rectangular filling matrix describing how  $N$  particles can be combined into  $L$  single-particle energy levels to generate the many-body states. The starting point of our method relies on the singular value decomposition of this matrix, which allows to expand the many-body spectrum as a weighted sum of 'principal' spectra. These spectra are universal and depend only on the number of single body levels and the number of particles. The weighting factors involve a discrete Fourier transformation of the single body energies, providing renormalized energies. Our approach is illustrated in the case of spinless non-interacting fermions, and applied to the tight-binding model in one and two dimensions, and to the

---

\* Correspondence email address: gregoire.ithier@rhul.ac.uk

transverse Ising field chain.

We organize the paper as follows. In Sec. II, we introduce the idea of principal analysis decomposition of a filling matrix and explain how it allows to access a Many Body spectrum. In Sec. III, we develop the method in the case of spinless fermions, discuss how to explore symmetries of the problem of calculating the MBDoS. Applications to tight-binding and Ising chains are discussed in Sec. IV. Finally, our main findings are summarized in Sec. V. We also provide appendixes with detailed analytical calculations used in the main text.

## II. PRINCIPAL COMPONENTS APPROACH

We start by considering a system for which we know the single-body spectrum, a discrete set of  $L$  energy levels with energies  $\epsilon_\ell$ . Our goal is to construct the many-body spectrum, which has energies  $E_p = \sum_\ell \epsilon_\ell n_\ell^p$ , where the occupation numbers  $n_\ell^p$  define the  $p$ -th many-body state, i.e. a configuration of particles dispatched over the single body levels. Our first step is to rewrite all those energies in matrix form by collecting all single-body energies  $\epsilon_\ell$  into a vector  $\epsilon$ , all many body energies  $E_p$  into a vector  $E$ , and finally construct a rectangular matrix  $F$ , the "filling" matrix, which has all possible configurations of occupation numbers in each row. We write :

$$E = F\epsilon \quad (1)$$

The singular value decomposition (SVD) of  $F = V\Sigma U^T$  provides the principal component expansion :

$$F = \sum_{\ell=0}^{L-1} \sigma_\ell \tilde{v}_\ell \tilde{u}_\ell^T \quad (2)$$

where  $\tilde{u}_\ell$  are the orthonormal right-singular vectors (i.e. the columns of  $U$ ),  $\sigma_\ell$  are the singular values (i.e. the main diagonal of  $\Sigma$ ), and  $\tilde{v}_\ell$  are the orthonormal left-singular vectors (i.e. the columns of  $V$ ). To ease notations, in the following we will work with right-singular vectors which are already orthonormalized, denoted by  $u_\ell = \tilde{u}_\ell$  but with left-singular vectors which are not normalized such that  $v_\ell = \sigma_\ell \tilde{v}_\ell$ . Note that with these notations,  $u_\ell$  and  $v_\ell$  are related by  $v_\ell = F u_\ell$ . The many-body energies can be rewritten as :

$$E = \sum_{\ell=0}^{L-1} (u_\ell^T \cdot \epsilon) v_\ell = \sum_{\ell=0}^{L-1} \tilde{\epsilon}_\ell v_\ell \quad (3)$$

where we defined  $\tilde{\epsilon}_\ell = u_\ell^T \cdot \epsilon$ .

The many body spectrum now appears as a sum of "principal" *spectral* components given by the  $v_\ell$  vectors. These spectral components are weighted by the new effective energies  $\tilde{\epsilon}_\ell$  of a renormalized single-body spectrum. In particular, the form of  $u_\ell$  defines which of these energies contribute to the many-body spectrum. As we will discuss later, a very convenient choice is given by Fourier

modes obtained from the analytical solution for the eigenvectors of the circulant matrix  $F^T F$ . Depending on the band structure of the system, it is also possible that some renormalized energies vanish which allows the associated  $\ell$  modes to be discarded.

The problem of computing the many body spectrum is now split in two parts. The first part is to compute the renormalized single body spectrum only depending on the right singular part of the SVD (i.e.  $u_\ell$ ) which can be obtained analytically. The second part depends on the left singular part of the SVD (i.e.  $v_\ell$ ) and the singular values, which only contain information about the universal properties of many-body systems encoded in the combinatoric structure of the  $F$  matrix. That second part requires a statistical approach but can be efficiently computed for large system sizes by avoiding using the  $F$  matrix explicitly since its size scales exponentially with the number of levels and particles considered.

In the following, we provide a framework to compute the singular decomposition of  $F$  in the case of a system of non-interacting fermions with no other quantum number.

## III. SPINLESS FERMIONS

In the case of fermions without any additional quantum number, occupation numbers can only be 0 or 1, which are exactly the matrix components of  $F$ . Each row of the filling matrix  $F$  (i.e. some configuration of a many body state) is a binary string. All rows share the same amount of 1's, to account for the fixed number of particles  $N$ , there are a total of  $C_L^N$  many body state configurations and the filling matrix  $F$  has dimension  $(L \times C_L^N)$ .

### A. Right part of the SVD

Let's first turn our attention to the right-singular vectors  $u_\ell$  and the singular values  $\sigma_\ell$ . Both can be computed by looking at the eigen decomposition of the square matrix  $F^T F$  which has dimension  $(L \times L)$  and happen to have a very simple form : a circulant matrix with only 2 distinct values, see Appendix A. Circulant matrices are well known and can be diagonalized by using Fourier modes. Let  $\omega = e^{i2\pi/L}$ , then eigenvectors of  $F^T F$  which are the right-singular vectors  $u_\ell$  of  $F$  are given by :

$$u_\ell = \frac{1}{\sqrt{L}} \left( 1, \omega^\ell, \omega^{2\ell}, \dots, \omega^{(L-1)\ell} \right) \quad (4)$$

The eigenvalues of  $F^T F$  take the following form :

$$\lambda_\ell = C_{L-1}^{N-1} + C_{L-2}^{N-2} \sum_{k=1}^{L-1} \omega^{k\ell}$$

from which it is easy to show that only two distinct values can arise. After taking the square root to obtain singular

values of  $F$ , we get :

$$\begin{aligned}\sigma_0 &= \sqrt{N C_{L-1}^{N-1}} && \text{with multiplicity } 1 \\ \sigma_{\ell \geq 1} &= \sqrt{C_{L-2}^{N-1}} && \text{with multiplicity } L-1\end{aligned}\quad (5)$$

One can easily check that  $u_\ell$  vectors form orthonormal bases for both eigen spaces, the  $\ell = 0$  case matching the 1-dimensional eigen space spanned by  $u_0$  and the  $\ell \geq 1$  case matching the  $L-1$ -dimensional eigen space spanned by  $u_{\ell \geq 1}$ .

### B. Left part of the SVD

In order to compute the left-singular vectors  $v_\ell$ , we avoid dealing with the matrix  $FF^T$  which is very large, and prefer using the identity  $v_\ell = Fu_\ell$ . We can write the components of  $v_\ell$  as follows :

$$v_\ell^p = \sum_{k=0}^{L-1} F_{p,k} \omega^{k\ell}$$

essentially, the inner product between  $u_\ell$  and the configuration of the  $p^{\text{th}}$  many body state. In other words, each component  $v_\ell^p$  of the left-singular vector is the discrete  $\ell^{\text{th}}$  Fourier coefficient of the binary string representing the occupation numbers of the  $p^{\text{th}}$  many body state.

We will now investigate two symmetries which provide a good understanding of universal properties of  $F$  and allow to reduce the very large set of configurations to a much more manageable size for numerical applications.

### C. The $k$ -symmetry

The first symmetry we observe is on the  $u_\ell$  vectors containing Fourier modes based on  $L^{\text{th}}$  roots of unity. Since they contain components of the form  $\omega^{k\ell}$ , it becomes clear that when taking the inner product of  $u_\ell$  against a configuration represented by a binary string, a circular permutation of those bits will only multiply the Fourier modes by a power of  $\omega$ , i.e. it will rotate the result  $v_\ell^p$  in the complex plane by a phase which is a power of  $\omega^\ell$ . We will denote this important angle  $\theta_{\text{step}} = 2\pi\ell/L$ . Note that it does not depend on  $N$  and stays valid for all components of a given  $v_\ell$ . It follows that all the components of  $v_\ell$  will lie on various circles in the complex plane, all of them having a relative angle which is a multiple of  $\theta_{\text{step}}$  between them. We call this structure the  $k$ -symmetry.

The  $k$ -symmetry suggests to group configurations together in equivalence classes defined by the underlying relation of circular permutations. Each class contains configurations that can be transformed into each other by circular permutation, we choose the lowest of them in lexicographic order as class representatives which we will refer to as "seeds". All members of such an equivalence class, when taking the inner product with  $u_\ell$ , will

produce  $v_\ell$  components which lie on the same circle in the complex plane, for any fixed given  $\ell$ . Note that two distinct classes can still map to the same circle by having the same radius.

There will be two kind of such equivalence classes : the non-degenerate classes contain exactly  $L$  binary strings when the bits don't provide any additional symmetry, while the degenerate classes contain less than  $L$  strings as the bits expose a shorter pattern that repeats under circular permutation, for instance  $(0, 0, 1, 1, 0, 0, 1, 1)$  is an 8-bits sequence but loops back early with a circular permutation by 4 positions. This distinction will become important later on.

Next, we notice that equivalence classes are closely related to the factors of  $L$ . In particular, if  $L$  is a prime number, all classes are non-degenerate. Degenerate classes can only have a cardinal which has a common factor with  $L$ . This can be deduced from the action of circular permutations on strings of various sizes. This is of particular physical meaning : the prime decomposition of  $L$  is a decisive feature for the symmetries of the filling matrix.

Finally, a counting argument can be made about those equivalence classes by using the Pólya enumeration theorem, from which we can estimate the number of equivalence classes to be of the order of  $C_L^N/L$ .

### D. The $\ell$ -symmetry

On the other hand, we can look at what happens when we consider a different Fourier coefficient and go from some  $v_\ell$  to another  $v_{\ell'}$ .  $u_\ell$  is changed component by component according to :  $u_{\ell'}^k = \omega^{k(\ell'-\ell)} u_\ell^k$ . We want to characterize a situation where the components of  $u_{\ell'}$  are simply a permutation of the components of  $u_\ell$ . This can be written formally :

$$\forall k \in \{0, L-1\}, \exists p, n \in \mathbb{Z} / \omega^{k(\ell'-\ell)} = \omega^{p\ell+nL}$$

from which we solve for the integer  $p$  :

$$p(k, n) = -k + \frac{k\ell' - nL}{\ell}$$

which means that  $\ell$  must divide  $(k\ell' - nL)$  when  $n$  is chosen while making sure that every component of  $u_\ell$  is mapped to another component in a one-to-one way. It can be shown that an equivalent condition to the above is given from greatest common divisors (gcd) :

$$\text{gcd}(L, \ell) = \text{gcd}(L, \ell') \quad (6)$$

In this case, since the permutation of  $u_\ell$  components is equivalent to the permutation of configurations in the  $F$  matrix, then vectors  $v_\ell$  and  $v_{\ell'}$  are also the same up to a permutation, i.e. the distributions of their components are identical. We call this property the  $\ell$ -symmetry.

In order to proceed, we need to introduce the language of compositions. A composition of an integer is similar to a partition, but with order taken into account.

Given some integer  $n$ , we subdivide  $n$  into  $p$  non-zero integer parts such that the sum of all parts is  $n$ . Any such sequence is called a  $p$ -composition of  $n$ . If we allow some of the  $p$  parts to be zero, then we call it a weak  $p$ -composition of  $n$ . Finally, if we also impose some integer  $k$  such that any part can only have a maximum value of  $k$ , then we call it a  $k$ -restricted weak  $p$ -composition of  $N$ .

The  $\ell$ -symmetry simplifies the study of the principal spectra, as only a small amount of  $\ell$  values are required to obtain the complete set of  $v_\ell$ , namely the divisors of  $L$ . To implement this, we can change our point of view on binary strings, and consider them as 1-restricted weak  $L$ -compositions of the integer  $N$ . We then proceed by considering only the  $\ell$ 's which divide  $L$ , and introduce the integer  $q = L/\ell$ . We subdivide each binary string into  $\ell$  parts of size  $q$ , and add them together component by component, effectively folding them into a vector of size  $q$ . We obtain  $\ell$ -restricted weak  $q$ -compositions of the integer  $N$ . This leads to the following simplification for Fourier coefficients :

$$v_\ell^p = \sum_{k=0}^{q-1} \left( \sum_{s=0}^{\ell-1} F_{p,sq+k} \right) e^{i2\pi \frac{k}{q}}$$

from which we redefine effective vectors  $u'_\ell$  of size  $q$ , which now contain Fourier modes based on the  $q^{\text{th}}$  roots of unity  $\omega' = e^{i2\pi/q}$ . Its components are of the form  $\omega'^k$  with  $k \in \{0, q-1\}$ .

Once again, we see that the divisors of  $L$ , i.e. its prime decomposition, plays a central role. In particular, if  $L$  is prime, we only need to compute the  $\ell = 1$  case where the  $\ell$ -symmetry is trivial and the  $\ell$ -restricted weak  $q$ -compositions are the binary strings themselves. There is also an interesting feature which can be observed from Fig.1, where increasing  $\ell$  values lead to a fast decreasing density of  $v_\ell$  components in the complex plane, while the occurrence counts of each points necessarily goes up : we transition from a spread distribution to a clustered distribution, i.e. with larger degeneracies.

### E. Enumeration and statistics

Both symmetries described above allow to simplify the study of the problem, but we must be careful about which one should we apply first. As we will point out soon, there is a strong incentive to use the  $\ell$ -symmetry first. Going from the set of  $C_L^N$  binary strings to a set of  $\ell$ -restricted weak  $q$ -compositions is an injective operation, so we should be careful to track down occurrence numbers. From the previous section, we see that a large number of distinct binary strings are mapped to the same composition. Let's denote by  $\{m_0, \dots, m_{q-1}\}$  the parts of an  $\ell$ -restricted weak  $q$ -composition, with  $m_k \in \{0, \ell\}$  and their sum adding up to  $N$ . Then, the total number of binary strings mapped to the same composition is given

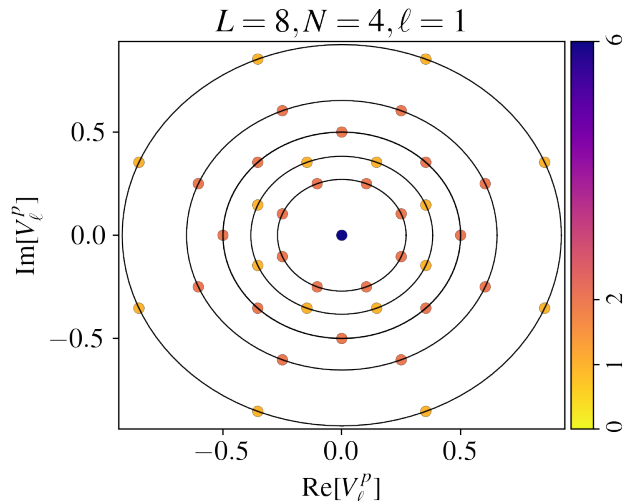


Fig. 1. **First principal spectrum  $v_1$  of the filling matrix  $F$  for  $L = 8$  and  $N = 4$ .** Each point is a distinct value of the distribution of the components of  $v_1$  in the complex plane. Circles relate components belonging to one or more equivalence classes with the same modulus. The number of occurrences of each values are : 6 (dark purple) for all degenerate classes with radius 0, 1 (yellow) which have 1 non-degenerate class per circle, and 2 (dark orange) which have 2 non-degenerate classes per circle.

by a winding factor :

$$Q = \prod_{k=0}^{q-1} C_\ell^{m_k} \quad (7)$$

From this point on, all "packed" configurations are now represented by a choice for each of the  $m_k$  values and we use  $u'_\ell$  vectors of size  $q$  containing  $q$ -roots of unity  $\omega'^k$  for  $k \in \{0, q-1\}$ . For notation simplicity, we will now drop the primes and simply redefine  $u_\ell$  and  $\omega$ .

The next step is to apply the  $k$ -symmetry on top of compositions, by again noticing that any circular permutation of a composition is only a multiplication of  $u_\ell$  by a power of  $\omega$  : we group compositions together in equivalence classes related by circular permutations. This is where an interesting feature comes in : by applying the  $k$ -symmetry on compositions, it can be shown that configurations inside degenerate classes will always have a null projection on the Fourier modes of  $u_\ell$ . We only need to count them to obtain the occurrence count of zero components in  $v_\ell$ .

We now have all the tools required for our framework. We can describe a simple recipe to obtain the exact distribution of all  $v_\ell$  vectors. First, we look at the value of  $L$  and construct the list of all its divisors : this gives us the  $\ell$  values we have to deal with. For each of them, we compute  $q = L/\ell$  and proceed in building the list of seeds : all  $\ell$ -restricted weak  $q$ -compositions which are not related by circular permutation. For each seed, we first look at the size of its equivalence class. If it is degenerate, i.e. lower than  $q$ , then the class lies on a 0-radius "circle" which is

a point at origin in the complex plane. In this case, we only need to recover the occurrence count which is the winding factor  $Q$  from Eq.(7) times the degenerate class size. Otherwise, the class is non-degenerate and has size  $q$ : the total occurrence count is  $Q$  times  $q$ , each vertex having an occurrence count of  $Q$ . We also compute the inner product of the seed with  $u_\ell$  directly and extract the module and argument of the result. The module needs to be normalized by  $1/\sqrt{\ell}$  to give us the radius of this seed's circle. The argument gives us one point on the circle from which we can reconstruct all other points coming from this seed's equivalence class by using increments of  $\theta_{\text{step}}$ , ie. the  $k$ -symmetry. We now know everything about that particular seed and its class. While processing all unique seeds and classes, we accumulate the ones found to lie on the same circle, ie. having the same radius, and simply add up occurrence counts accordingly. The end result is a list of all the circles, their respective radius, point angular positions if needed, and occurrence numbers (by point or by circle, whichever is needed). This gives the exact distribution of  $v_\ell$ . Finally, all other  $\ell$  values which were skipped are recovered from  $\ell$ -symmetry by the criteria from Eq.(6).

The number of seeds to enumerate is much smaller than the initial set of binary strings, which makes a direct approach viable for decently large systems, ie.  $L$  of the order of 100. Even larger systems can be computed by adding a statistical layer on top of that by only selecting a sample set of uniformly chosen seeds. Once an exact or good enough approximation of the distribution of  $v_\ell$  components is known,  $v_\ell^p$  is simply treated as a random variable following that distribution. From those, we can sample many-body energies to construct the many-body spectrum and are ultimately able to obtain its density of state.

#### IV. APPLICATIONS: SPINLESS FERMIONS

A variety of systems can be described in terms of spinless fermions, including hard core bosons [19], Mott insulators in ladders [20], spin liquids [21], and, very recently, they served as the basis to study topological phases [22] and systems supporting Majorana fermions [23, 24].

To illustrate our method, we will apply it to two classes of problems: (i) tight-binding describing electrons interacting in a one-dimensional chain and in a square lattice, (ii) and to the transverse Ising field chain that describes a critical 1D spin chain, and which can be mapped into a single-particle problem using the Jordan Wigner (JW) transformation. In both, we consider periodic boundary conditions (PBC).

In the case (i), the Hamiltonian reads

$$H = -t \sum_{\langle i,j \rangle} (c_j^\dagger c_j + \text{H.c.}), \quad (8)$$

where the sum  $\langle i,j \rangle$  runs over first-neighbor sites,  $c_i/c_i^\dagger$

are the annihilation/creation operators, and  $t$  is the hopping amplitude. In 1D, the single-body energies are

$$\epsilon_k = -2t \cos(k), \quad (9)$$

the momenta  $k$  depends on the boundary conditions of the model. For periodic boundary conditions (PBC)  $k = \frac{2\pi n}{L}$ , with  $n = 0, \dots, L-1$ .

The trigonometric form of the dispersion relation associated with the fact that the matrix Hamiltonian is circulant has an interesting implication to the renormalized energies in Eq.(3). The periodicity shared between the single-body energies and the Fourier modes allows for the cancellation of all renormalized energies  $\tilde{\epsilon}_\ell$  except those associated with  $\ell = 1$  and  $\ell = L-1$ , which are symmetric to each other. We can show that these surviving contributions are equal to  $\tilde{\epsilon}_1 = \tilde{\epsilon}_{L-1} = -t\sqrt{L}$ . This result is illustrated in Fig. 3

In 2D, the band structure contains  $L^2$  single-body energies given by

$$\epsilon_{k_x, k_y} = -2t \cos(k_x) - 2t \cos(k_y), \quad (10)$$

where the momenta in each direction are  $k_x = \frac{2\pi n_x}{L}$  and  $k_y = \frac{2\pi n_y}{L}$ , with  $n_x, n_y = 0, \dots, L-1$ .

Similarly to the one-dimensional case, the renormalized band structure of the square lattice will be non-null for only a few  $\ell$ 's, due to the high degeneracy of the single-body energies. In particular,  $\epsilon_{k_x, k_y} = 0$  has degeneracy  $2(L-1)$ , whereas the only non-degenerate energies occur at the bottom and at the top of the band, where  $\epsilon_{k_x, k_y} = -4J$  and  $\epsilon_{k_x, k_y} = 4J$ , respectively. By flattening the 2D band structure as a 1D vector with  $L^2$  entries, one can show that the  $\tilde{\epsilon}_\ell$  do not vanish for  $\ell = nL + 1, n = 0, 1, \dots, L/2 - 1$  and  $\ell = mL - 1, m = 1, 2, \dots, L/2$ , and for  $\ell = L$ , which is a special case in which  $\tilde{\epsilon}_\ell$  is real. The band structure in eq. (10) and the non-vanishing renormalized energies  $\tilde{\epsilon}_\ell$  for a square lattice with  $L = 100$  sites is shown in Fig. 4. The real part decays fast with  $\ell$ , while the imaginary part converges to a constant, with oscillations decreasing with  $\ell$ .

In the case (ii), the Hamiltonian is

$$H = -J \sum_j \sigma_j^x \sigma_{j+1}^x - h \sum_j \sigma_j^z, \quad (11)$$

where  $\sigma^d$   $d = x, y, z$  are the Pauli matrices,  $J$  is the couplings and  $h$  is the transverse field.

The critical point occurs at  $h = J$ . After employing the JW transformation, we can obtain the dispersion relation of this model as follows

$$\epsilon_{k_\pm} = \pm 2J \sqrt{h^2 + 1 - 2h \cos(k)} - 2Jh, \quad (12)$$

with  $k = \frac{2n\pi}{L}$  and  $n = 0, \dots, L-1$  being the momentum. Note that now, two bands, one positive and other negative, contribute to the density of states.

In this case, the structure of the momenta  $k$  corresponding to the Fourier modes result in most of the

renormalized energies to be non-zero, however only odd indexes contribute. For the real part, all  $\text{Re}[\tilde{\epsilon}_\ell] = 4/\sqrt{2L}|h/J - 1|$  with odd  $\ell$ , independent of  $\ell$ . The factor in modulus introduces a symmetry around the critical point  $h_c = J$ , so that  $\tilde{\epsilon}_\ell[h - h_c < 0] = \tilde{\epsilon}_\ell[h - h_c > 0]$ . For the imaginary part, the  $\text{Im}[\tilde{\epsilon}_\ell]$  associated with  $l$  indexes are non-zero, but they decay very fast. The decay rate is amplified as the system size increases. At the critical point  $h = J$ , the only surviving single-body energies are  $\tilde{\epsilon}_{\ell=1} = -\tilde{\epsilon}_{\ell=L-1} = 2i\sqrt{2L}$ .

This can be observed in Fig. 5, panel (b), where we show the real and imaginary parts of  $\tilde{\epsilon}_\ell$  for  $h/J \in [0.5, 1.5]$ .

Using these previous results, we have all ingredients to compute the MBDoS for the applications aforementioned. Basically, we need the number of occurrences of the components of relevant  $v_\ell$ 's multiplied by the non-vanishing renormalized single-body energies. The result for a tight-binding chain is shown in Fig. 6

## V. CONCLUSION

In the present paper, we explored a novel approach to compute the many-body density of states of quantum systems whose Hamiltonian can be mapped into non-interacting spinless fermions.

We show that the many-body spectrum can be expanded over the principal components of a filling matrix encoding the allowed many body states. These principal components describe universal spectral properties of systems of spinless fermions, only depending on the numbers of particles and single body levels. This new spectral decomposition of many body states is weighted by a renormalized single body band structure, which acts as a filter for relevant energy scales.

For gapless systems, such as the tight-binding and the critical transverse field Ising chains, we demonstrated that only two renormalized energies are non zero. Even in more general scenarios, such as the square lattice or the Ising chain away from the critical point, many renormalized energies still vanish. In all cases, this significantly reduces the number of relevant spectral components of the filling matrix involved in the calculation of the many body density of states.

Our framework can be extended to include additional quantum numbers like spin, and to handle bosonic systems.

### Appendix A: Computing the SVD of F

As stated in the main text, the core of the method relies on computing the SVD of the filling matrix  $F$ . Start-

ing from the simplest case of spinless fermions, the  $F$  matrix contains configurations in each row which are simply binary strings of 0s and 1s. It also has the property that every row contains the same amount of 1s, the fixed number of particles  $N$ . Finally, all columns also contains the same number of 1s, as a consequence of combinatorics. To compute the SVD, we start by looking at the eigen decomposition of  $F^T F$  which can be done analytically. When computing matrix elements of  $F^T F$  as scalar products of columns against other columns, only 2 things can happen. In the first case, a column is matched against itself, giving the diagonal of  $F^T F$ , and simple combinatorics tells us that there will be  $C_{L-1}^{N-1}$  matching 1s since there is one fixed level with a particle when looking at row configurations. In the second case, one columns is matched with a different one, giving off-diagonal elements of  $F^T F$ , this time the same logic tells us that there will be  $C_{L-2}^{N-2}$  matching 1s between them since there are now 2 different fixed levels with a particle when looking at row configurations. From this reasoning we deduce that the  $F^T F$  matrix has a very simple form :

$$F^T F = \begin{pmatrix} a & b & \dots & b \\ b & \ddots & & \vdots \\ \vdots & & \ddots & b \\ b & \dots & b & a \end{pmatrix}_{L \times L}$$

where  $a = C_{L-1}^{N-1}$  and  $b = C_{L-2}^{N-2}$  for clarity. This is a very simple case of a circulant matrix which only has 2 distinct values. Its characteristic polynomial is easily factorized in the following form :

$$P_{F^T F}(\lambda) = (a + (L-1)b - \lambda)(a - b - \lambda)^{L-1}$$

from which one can easily compute both eigenvalues and their multiplicity before taking the square root to obtain the singular values of  $F$  given in the main text in Eq.(5).

Regarding the eigenvectors, we have a choice of basis to make, which will influence greatly how we proceed for the next step which is to compute the left-singular vectors  $v_\ell$ . There are basically two natural choices here. First, we can go ahead and solve the linear system which happens to be simple, before using a standard Gram-Schmidt orthonormalization procedure. This method allows to compute the distribution of corresponding  $v_\ell$  components exactly but in a form that is not so easy to deal with, while also making physical interpretations quite difficult due to the lack of structure in how information is encoded. Secondly, we can use the property of circulant matrices which allow to express their eigenvectors with Fourier modes using  $L$ -roots of unity. Computing the distribution of  $v_\ell$  components exactly is quite harder as we will see, but the information structure is much cleaner thanks to Fourier analysis. The latter is the method we ultimately chose.

- 
- [1] V. Zelevinsky and M. Horoi, *Progress in Particle and Nuclear Physics* **105**, 180 (2019).
- [2] N. Ashcroft, A. W. Mermin, N. Mermin, and B. P. Company, *Solid State Physics*, HRW international editions (Holt, Rinehart and Winston, 1976).
- [3] C. Gogolin and J. Eisert, *Reports on Progress in Physics* **79**, 056001 (2016).
- [4] L. F. Santos and M. Rigol, *Phys. Rev. E* **81**, 036206 (2010).
- [5] F. Borgonovi, F. Izrailev, L. Santos, and V. Zelevinsky, *Physics Reports* **626**, 1 (2016), quantum chaos and thermalization in isolated systems of interacting particles.
- [6] A. Polkovnikov, K. Sengupta, A. Silva, and M. Vengalattore, *Rev. Mod. Phys.* **83**, 863 (2011).
- [7] R. Nandkishore and D. A. Huse, *Annual Review of Condensed Matter Physics* **6**, 15 (2015), <https://doi.org/10.1146/annurev-conmatphys-031214-014726>.
- [8] D. A. Abanin, E. Altman, I. Bloch, and M. Serbyn, *Rev. Mod. Phys.* **91**, 021001 (2019).
- [9] G. Ithier and F. Benaych-Georges, *Phys. Rev. A* **96**, 012108 (2017).
- [10] G. Ithier, S. Ascroft, and F. Benaych-Georges, *Phys. Rev. E* **96**, 060102 (2017).
- [11] A. Weiße and H. Fehske, in *Computational many-particle physics* (Springer, 2008) pp. 529–544.
- [12] A. Weiße, G. Wellein, A. Alvermann, and H. Fehske, *Rev. Mod. Phys.* **78**, 275 (2006).
- [13] H. A. Bethe, *Phys. Rev.* **50**, 332 (1936).
- [14] A. Volya and V. Zelevinsky, *Phys. Rev. C* **74**, 064314 (2006).
- [15] M. Hillman and J. R. Grover, *Physical Review* **185**, 1303 (1969).
- [16] J. Berger and M. Martinot, *Nuclear Physics A* **226**, 391 (1974).
- [17] C. Jacquemin and S. Kataria, *Zeitschrift für Physik A Atomic Nuclei* **324**, 261 (1986).
- [18] A. N. Bohr and B. R. Mottelson, *Nuclear Structure (in 2 volumes)* (World Scientific Publishing Company, 1998).
- [19] M. Girardeau, *Journal of Mathematical Physics* **1**, 516 (1960), <https://doi.org/10.1063/1.1703687>.
- [20] P. Donohue, M. Tsuchiizu, T. Giamarchi, and Y. Suzumura, *Phys. Rev. B* **63**, 045121 (2001).
- [21] A. Imambekov, T. L. Schmidt, and L. I. Glazman, *Rev. Mod. Phys.* **84**, 1253 (2012).
- [22] A. M. Turner, F. Pollmann, and E. Berg, *Phys. Rev. B* **83**, 075102 (2011).
- [23] A. Y. Kitaev, *Physics-Uspekhi* **44**, 131 (2001).
- [24] J. Alicea, *Phys. Rev. B* **81**, 125318 (2010).

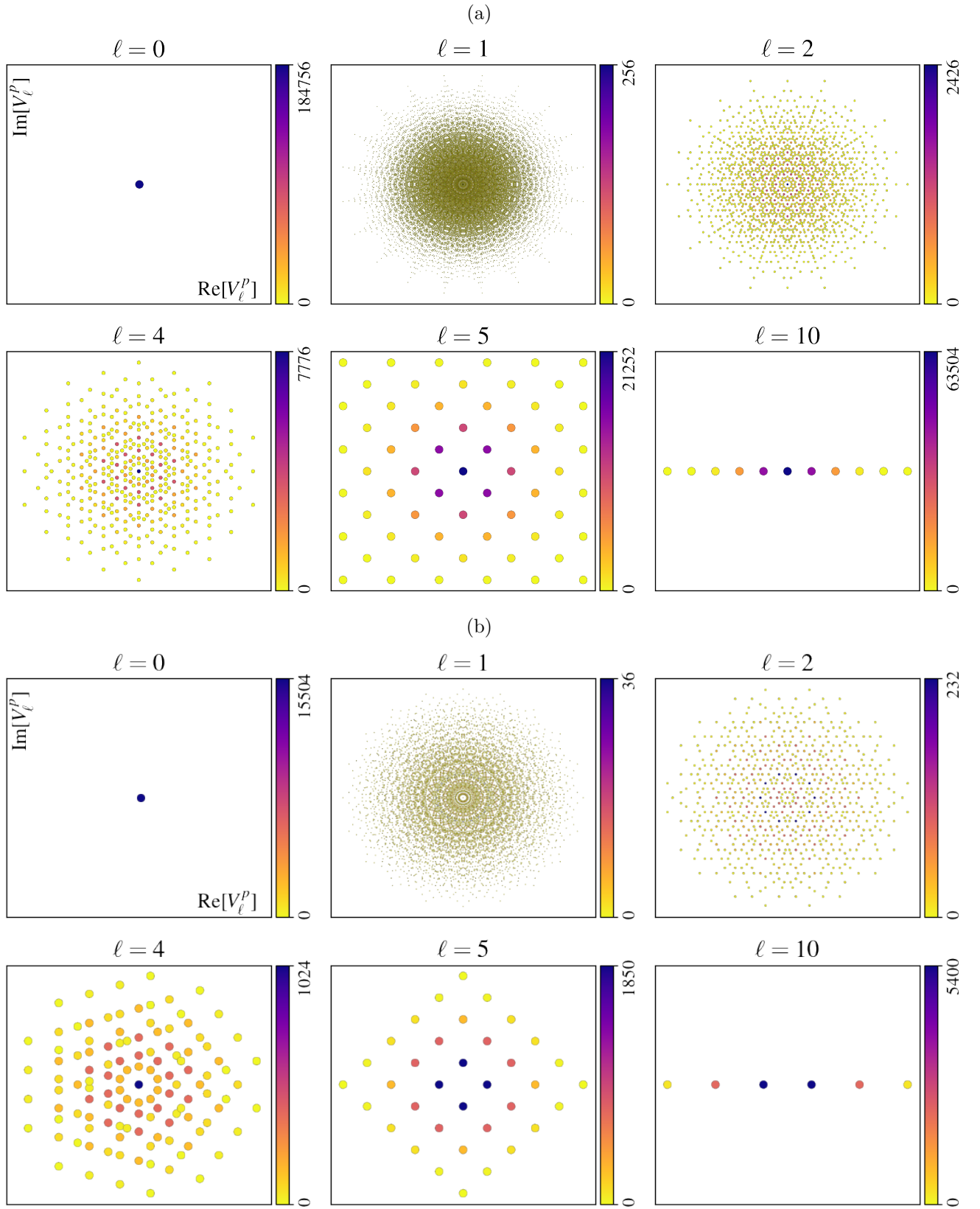


Fig. 2. **Principal spectra of the filling matrix  $F$  in the case  $L = 20$  at half-filling  $N = 10$  (a) or quarter-filling  $N = 5$  (b).** Each graph represents components of the  $v_\ell$  vector in the complex plane and their occurrence numbers. All relevant  $\ell$  values with distinct greatest common divisors with  $L$  are shown, other  $\ell$  values yield identical distributions through  $\ell$ -symmetry, according to the criteria from Eq.(6). The full set of  $\ell$  values spectra can be found in Fig. 7. The  $\ell = 0$  case is also shown and corresponds to the 1-dimensional eigenspace associated to the singular decomposition of  $F$ . One can notice that increasing values of  $\ell$  yield more clustered distributions.



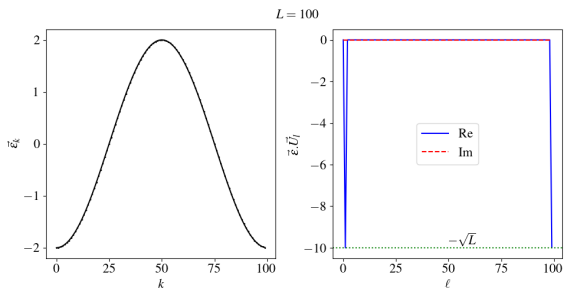


Fig. 3. **Band dispersion and renormalized single-body energies  $\tilde{\epsilon}_\ell$  for tight-binding models in a 1D chain of  $L = 100$  sites.** The only surviving renormalized energy  $\tilde{\epsilon}_\ell = -J\sqrt{L}$  are  $\ell = 1$  and  $\ell = L - 1$ .

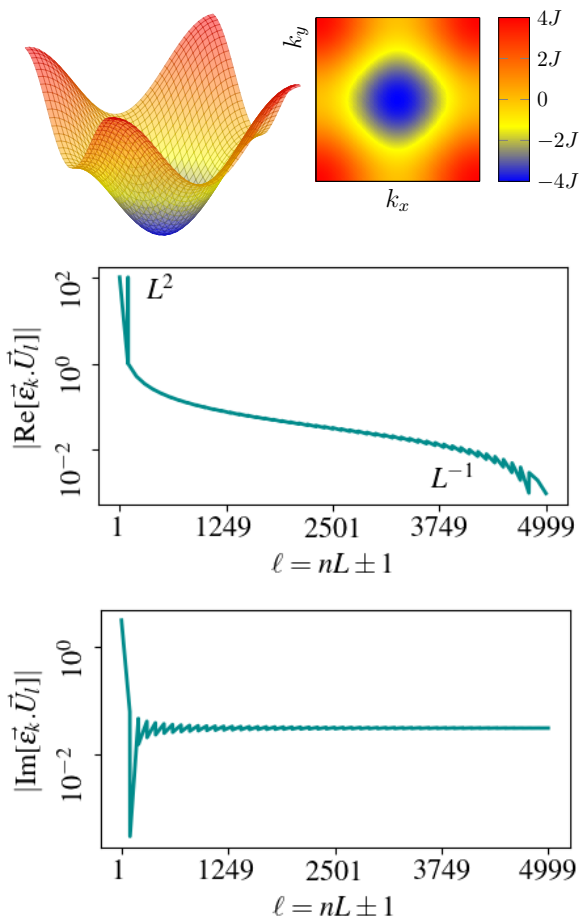


Fig. 4. **Band structure and renormalized energies of a homogeneous square lattice with  $L = 100$  sites in each direction.** Top panels show the single-body band structure  $\epsilon_{k_x, k_y}$  as a surface in 3D (left) and as a contourplot (right). Bottom panels display the real and imaginary part of the renormalized energies  $\tilde{\epsilon}_\ell$ . Note that only  $2(L+1)$  renormalized energies indexed as  $\ell = nL \pm 1$  do not vanish.

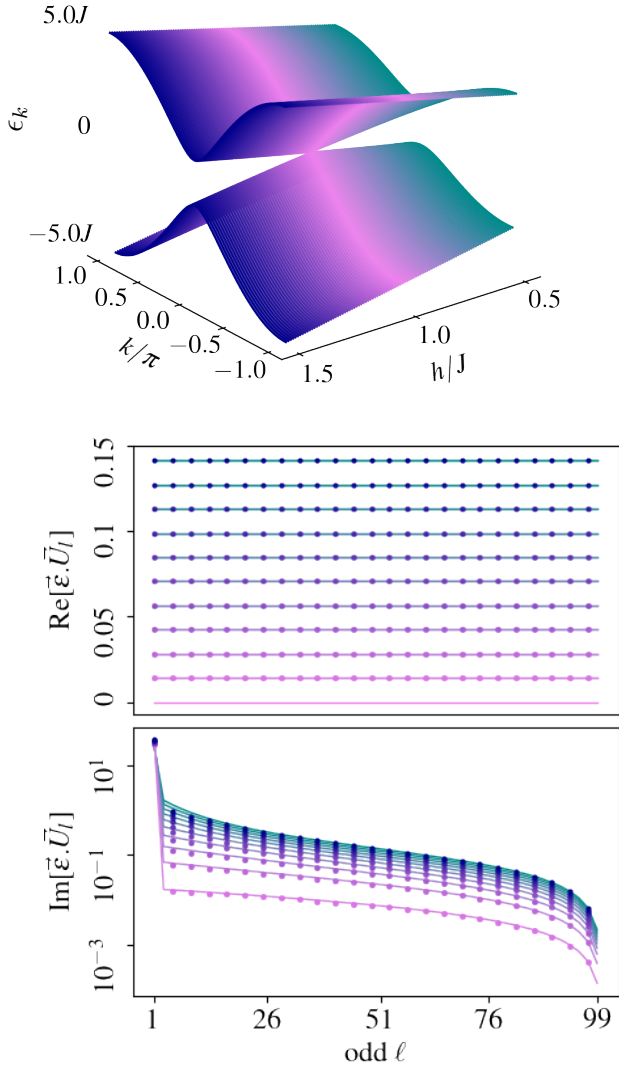


Fig. 5. **Band structure and renormalized single-particle energies  $\tilde{\epsilon}_\ell$  for an Ising chain under a transverse field with strength  $h$ .** The number of sites/levels is  $L = 100$ . Top contour shows the band dispersion as a function of  $k$  and  $h$ . Bottom panels display the real and imaginary parts of the  $\tilde{\epsilon}_\ell$ 's for  $\ell$  odd. All components with  $\ell$  even vanish. The imaginary part decays as a function of  $\ell$ . Both real and imaginary parts are degenerate around  $h_c = J$ , i.e.  $\tilde{\epsilon}_\ell[h - h_c < 0] = \tilde{\epsilon}_\ell[h - h_c > 0]$ . At the critical point, the dominant renormalized energy is  $\tilde{\epsilon}_1$ , all other renormalized energies can be neglected in a first approximation. As a result, the MBDoS will be similar to the one of the 1D tight binding model.

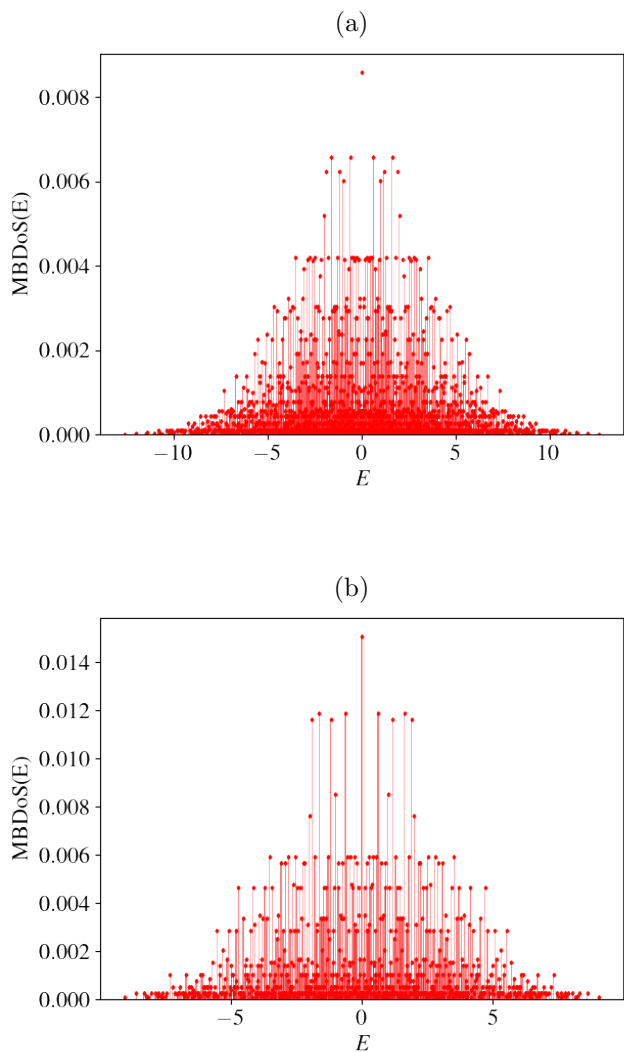


Fig. 6. **Many-body DoS for a 1D tight-binding chain with  $L = 20$  sites at half-filling  $N = 10$  (a), or quarter-filling  $N = 5$  (b).** These are obtained by applying Eq.3 where the only non-zero renormalized energies  $\tilde{\epsilon}_\ell$  are for  $\ell = 1$  and  $\ell = L - 1$  (see Sec. IV).

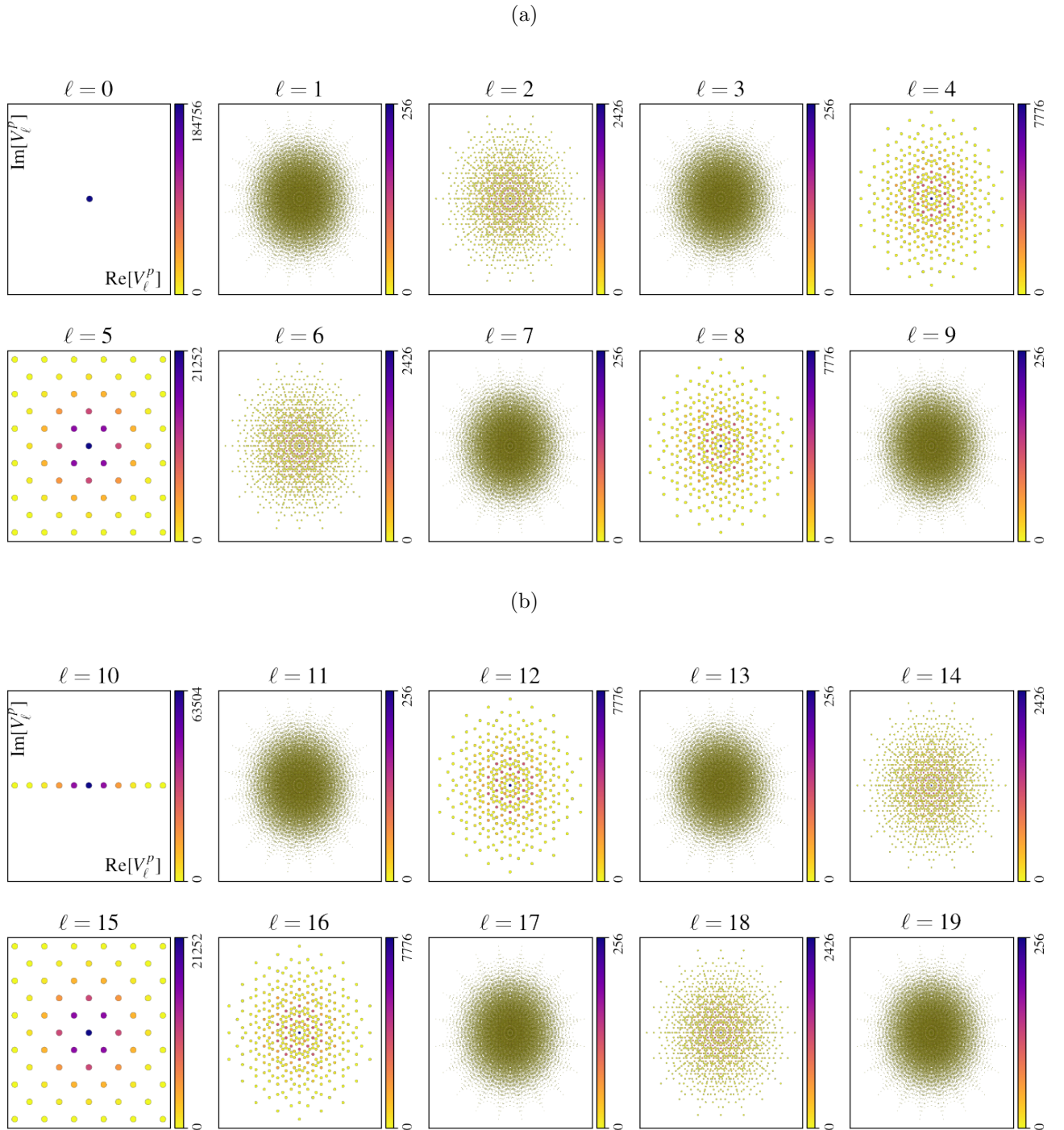


Fig. 7. Full spectrum of components of  $v_\ell$ 's for  $L = 20$  at half-filling  $N = 10$ . All  $\ell$  values with the same greatest common divisor with  $L$  have the same principal spectrum  $v_\ell$ , illustrating the  $\ell$ -symmetry discussed in Sec.III.